ISSN 0020-4412, Instruments and Experimental Techniques, 2010, Vol. 53, No. 1, pp. 15–28. © Pleiades Publishing, Ltd., 2010.
Original Russian Text © O.V. Anchugov, V.E. Blinov, A.V. Bogomyagkov, A.A. Volkov, A.N. Zhuravlev, S.E. Karnaev, V.A. Kiselev, E.B. Levichev, O.I. Meshkov, S.I. Mishnev, I.I. Morozov, N.Yu. Muchnoi, S.A. Nikitin, I.B. Nikolaev, V.V. Petrov, P.A. Piminov, E.A. Simonov, S.V. Sinyatkin, A.N. Skrinskii, V.V. Smaluk, Yu.A. Tikhonov, G.M. Tumaikin, V.M. Tsukanov, A.G. Shamov, D.N. Shatilov, D.A. Shvedov, 2010, published in Pribory i Tekhnika Eksperimenta, 2010, No. 1, pp. 20–33.

NUCLEAR EXPERIMENTAL TECHNIQUE

Use of the Methods of Accelerator Physics in Precision Measurements of Particle Masses at the VEPP-4 Complex with the KEDR Detector

O. V. Anchugov, V. E. Blinov, A. V. Bogomyagkov, A. A. Volkov, A. N. Zhuravlev, S. E. Karnaev, V. A. Kiselev, E. B. Levichev, O. I. Meshkov, S. I. Mishnev, I. I. Morozov, N. Yu. Muchnoi, S. A. Nikitin, I. B. Nikolaev, V. V. Petrov, P. A. Piminov, E. A. Simonov, S. V. Sinyatkin, A. N. Skrinskii, V. V. Smaluk, Yu. A. Tikhonov, G. M. Tumaikin, V. M. Tsukanov, A. G. Shamov, D. N. Shatilov, and D. A. Shvedov

Budker Institute of Nuclear Physics, Siberian Branch, Russian Academy of Sciences, pr. Akademika Lavrent'eva 11, Novosibirsk, 630090 Russia

Received May 26, 2009

Abstract—Based on precision measurements of the beam energy using the resonant depolarization and Compton backscattering methods, it is possible to conduct high-precision experiments in the field of high-energy physics at the VEPP-4M electron–positron collider with the KEDR detector. The J/ψ- and $\psi(2s)$-meson masses measured at the VEPP-4M collider are among the ten most precisely known masses of elementary particles measured over the whole physical history. The degree of accuracy that we attained in determining the τ-lepton mass by the threshold behavior of the $e^+e^- \longrightarrow \tau^+\tau^-$ reaction cross section is the best in the world. Systems automatically controlling the temperature of the distillate that cools the magnets of the main accelerating structure and the RF accelerating cavities of the VEPP-4M collider have been developed, produced, and placed in operation in order to increase the efficiency of the complex. Simultaneous measurements of the transverse displacement and the angle of inclination of the beam near the interaction point can be taken with the aid of a multipinhole X-ray camera.

DOI: 10.1134/S0020441210010021

INTRODUCTION

The VEPP-4 accelerating complex, which includes an injector, the VEPP-3 booster storage ring, and the VEPP-4M electron–positron collider with the KEDR versatile magnetic detector, has been designed for experiments with colliding electron–positron beams [1]. The VEPP-4M is an upgraded collider, which has been used in high-energy physical experiments since 1977. The upgrading has made it possible to substantially increase its luminosity.

The KEDR detector [2] is a versatile magnetic detector for high-energy physical experiments in the energy range of 2–11 GeV in the center-of-mass system. The KEDR detector contains the following main systems: a vertex detector, a drift chamber, aerogel Cherenkov counters, time-of-flight scintillation counters, an electromagnetic calorimeter based on liquid krypton, an endcap electromagnetic calorimeter based on CsI crystals, a superconducting magnetic coil, a muon system, a system for detecting scattered electrons, and a luminosity monitor.

The results of the experiments carried out on the VEPP-4 complex with the aim of precision measurements of particle masses are presented in Table 1.

Since 2002, the VEPP-4 complex has been used to conduct high-energy physical experiments in the beam energy range of 0.9–2.0 GeV. At low energies such as these, the peak luminosity of the VEPP-4M electron–positron collider is $(1.0–2.5) \times 10^{30}$ cm^{-2} s^{-1} and the average rate of acquiring the luminosity integral is 300 nb^{-1} per week. The graph of the increase in the luminosity integral in 2004–2008 is shown in Fig. 1.

Though the VEPP-4M is inferior to modern colliders in luminosity, nevertheless, the VEPP-4 complex with the KEDR detector possesses a number of advantages, among which the following ones are of prime importance:

—the energy range of 0.9–5.5 GeV in the beam, which is unique for the available machines;

—the capability of measuring the beam energy using the resonant depolarization method with a record-braking relative accuracy of 10^{-6}, which has not been attained in any other laboratory in the world;

Table 1. High-energy physical experiments on the VEPP-4 complex

Particle	Energy, MeV	Relative accuracy	Detector	Years
J/ψ	3096.93 ± 0.10	3.2×10^{-5}	OLYa	1979–1980
$\psi(2s)$	3685.00 ± 0.12	3.3×10^{-5}	OLYa	1979–1980
Υ	$9460.57 \pm 0.09 \pm 0.05$	1.2×10^{-5}	MD-1	1983–1985
Υ'	10023.5 ± 0.5	5.0×10^{-5}	MD-1	1983–1985
Υ''	10355.2 ± 0.5	4.8×10^{-5}	MD-1	1983–1985
J/ψ	$3096.917 \pm 0.010 \pm 0.007$	3.5×10^{-6}	KEDR	2002–2005
$\psi(2s)$	$3686.119 \pm 0.006 \pm 0.010$	3.0×10^{-6}	KEDR	2002–2005
$\psi(3770)$	$3772.9 \pm 0.5 \pm 0.6$	2.1×10^{-4}	KEDR	2002–2005
D^0	$1865.43 \pm 0.60 \pm 0.38$	3.8×10^{-4}	KEDR	2002–2005
$D^{\pm}$	$1863.39 \pm 0.45 \pm 0.29$	2.9×10^{-4}	KEDR	2002–2005
τ	$1776.69^{+0.17}_{-0.19} \pm 0.15$	1.3×10^{-4}	KEDR	2005–2007

—the possibility of continuously monitoring the beam energy with a relative accuracy of 5×10^{-5} and the energy spread with an accuracy of 10% by measuring the position of the Compton edge in the spectrum of backscattered monochromatic laser photons; and

—the parameters of the KEDR versatile magnetic detector, which is part of the complex, are comparable to those of modern detectors for experiments at electron–positron colliders; the distinctive features of the KEDR are as follows: a system for detecting scattered electrons and positrons with a record-breaking resolution of 10^{-3}, an electromagnetic calorimeter based on liquid krypton capable of measuring the coordinate of a γ-ray conversion point with an accuracy of 1 mm, and a system of aerogel Cherenkov counters.

The system for measuring the particle energy using the resonant depolarization method and the procedure for energy reconstruction between calibrations with the use of measured VEPP-4M parameters, which we developed and tried out, allow us to measure particle masses with an extremely high accuracy. Thus, the measurement accuracy for the J/ψ- and

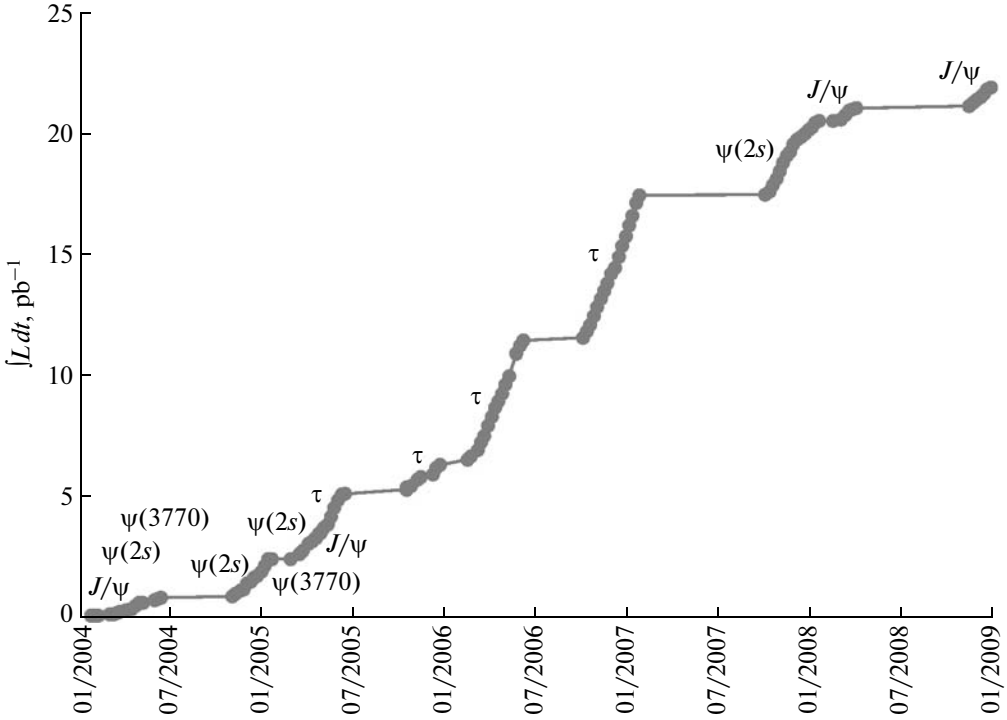

Fig. 1. Luminosity integral recorded with the KEDR detector.

$\psi(2s)$-meson masses is three to four times better than the world-average value [3]. Today, only the electron, proton, neutron, muon, and $\pi^{\pm}$-meson masses have been measured with a higher accuracy.

In the experiment aimed at precisely measuring the mass of a τ lepton near its production threshold, acquisition of data was completed in 2008. The goal of this experiment was to determine the τ-lepton mass with a higher precision, whereas the knowledge of this mass, along with the knowledge of the lifetime and the probability of the τ-lepton decay into an electron, a neutrino, and an antineutrino, offers a chance to verify the hypothesis of lepton universality—one of the main postulates of the Vineberg–Salam theory of electroweak interactions. Processing of these experimental data makes it possible to obtain the τ-lepton mass with the highest degree of accuracy attainable today [4]:

$$\text{PDG 2006: } 1776.90^{+0.29}_{-0.26}\text{ MeV;}$$

$$\text{BES 1996: } 1776.96^{+0.31}_{-0.27}\text{ MeV;}$$

$$\text{BELLE 2006: } 1776.77^{+0.35}_{-0.35}\text{ MeV;}$$

$$\text{KEDR 2008: } 1776.69^{+0.23}_{-0.24}\text{ MeV.}$$

Physical experiments in the region of *c*-quark production are being continued. Preliminary results have been obtained in the measurements of masses of charged and neutral *D* mesons and $\psi(3770)$ meson with accuracies comparable to or higher than the world average values [3]. Neutral and charged *D* mesons are the lightest states with an open charm. It is important that the exact values of their masses be known, since they are a reference point for masses of excited states. In addition, measurements of their masses are necessary for understanding the nature of recently discovered state $X(3872)$, which is close in mass to the production threshold of a D^0–D^{*0} pair.

Until 2007, the world-average accuracy in measuring the *D*-meson masses was ~0.5 MeV and was basically determined by the most precise ACCMOR and MARK-II experiments. In 2007, the scientists of the CLEO-c collaboration measured the D^0 mass with an accuracy of 0.18 MeV from analysis of the $D^0 \longrightarrow K_s\varphi$ decay. In the experiment with the KEDR detector, we measured the masses of the neutral and charged *D* mesons. Our knowledge of the D^0-meson mass agrees with the more precise value obtained in another way during the CLEO-c collaboration, and the $D^{\pm}$-meson mass agrees with the world-average value, i.e., is the most precise direct measurement of the $D^{\pm}$-meson mass.

The $\psi(3770)$ resonance was discovered 30 years ago, but its theoretical description has not been clarified. Existing models predict resonance parameters differing from the experimental data. Three scans of the $\psi(3770)$ resonance were performed on the KEDR detector, and a total luminosity integral of ~2.40 pb^{-1} was acquired; as a result, the mass and the full width at half-maximum of this resonance were measured. Our measurement of the $\psi(3770)$ mass is the most precise.

BEAM ENERGY MEASUREMENTS

Precision measurements of the beam energy are a very important part of an experiment aimed at measuring the particle masses. Two techniques for measuring the beam energy are used today at the VEPP-4M collider: one is based on resonant depolarization (RD) of the beam, and the other on Compton backscattering (CBS).

The RD method is the most precise modern technique for calibrating the beam energy. Beam energy calibrations were regularly performed with record-breaking accuracy (up to 10^{-6}) in the course of the experiments with the KEDR detector. In the time intervals between the calibrations, the beam energy was calculated using the interpolation method and the measured VEPP-4M parameters.

Along with indubitable advantages, the RD technique has a number of drawbacks: it breaks the polarization state and does not permit taking of prompt measurements when the luminosity integral is acquired. Therefore, a system based on the CBS method was developed for prompt measurements of the beam energy. Though the accuracy of this method is worse (~3×10^{-5}), nevertheless, the measurement process takes less time and does not require beam polarization. In addition, measurements can be made directly during acquisition of the luminosity integral. The use of two approaches offers a chance to improve the reliability of experimental results and provide required accuracy. In this case, the energy is measured using the precise RD method at the beginning and end of data acquisition, and monitoring based on CBS is carried out in the course of acquisition.

Resonant Depolarization Method

The RD method for measuring the beam energy has been proposed and implemented for the first time at the Budker Institute of Nuclear Physics (BINP) [5]. This approach has been widely used thereafter both at the BINP and in other laboratories throughout the world.

In an accelerator with a flat orbit (when radial and longitudinal magnetic and electric fields, as well as a transverse magnetic field, are absent), the spin precesses around the direction of guiding magnetic field **B**. Calculating the spin phase shift over the particle's circulation period, we obtain the expression for the mean frequency Ω_s of spin precession

$$\Omega_s = \left(\frac{q_0}{\gamma} + q'\right)\frac{1}{2\pi}\oint B_{\perp}(\theta)d\theta = \omega_0\left(1 + \gamma\frac{q'}{q_0}\right), \qquad (1)$$

where θ is the azimuth along a closed orbit, ω_0 is the cyclic circulation frequency, γ is the relativistic factor,

and q_0 and q' are the normal and abnormal parts of the gyromagnetic ratio.

The RD method is based on precision measurement of spin precession frequency Ω_s. Depolarization is caused by introduction of an external electromagnetic field with frequency Ω_D satisfying the resonance condition

$$\Omega_s \pm \Omega_D = n\omega_0 \quad (2)$$

at any integer n. The fact of depolarization is detected by any polarization-sensitive process.

By introducing normalized spin frequency $\nu_s = \frac{\Omega_s}{\omega_0} - 1 = \gamma\frac{q'}{q_0}$, we obtain a simple equation for beam energy E:

$$E = \nu_s \frac{mc^2}{q'/q_0} = 440.64843(3)\,\text{MeV} \cdot \nu_s. \quad (3)$$

The constants included in this expression have been known with a high precision: $q'/q_0 = 1.1596521859 \times 10^{-3} \pm 3.8 \times 10^{-12}$, $mc^2 = 0.51099892 \pm 4 \times 10^{-8}$ MeV. This offers a chance in principle to determine the particle energy by the measured frequency of spin precession with a limiting relative accuracy of 7.8×10^{-8}.

Polarized electron–positron beams are produced in storage rings owing to the action of magnetic dipole radiation. As a particle moves, its magnetic moment precesses around the direction of the magnetic field vector and the field-orthogonal component of the magnetic moment is reduced by magnetic dipole radiation. As a result, the spin is aligned with the magnetic field over the characteristic radiation time (the Sokolov–Ternov effect).

Assuming that the orbit in the homogeneous magnetic field is circular, polarization time τ_{pol} [s] can be presented in terms of radius R [m] of the particle trajectory:

$$\tau_{pol} \cong \frac{R^3}{\gamma^5}\frac{1}{\lambda_e c r_0} = \frac{2.8 \times 10^{18} R^3}{\gamma^5}, \quad (4)$$

where $\lambda_e = \frac{\hbar}{m_e c} = 3.86 \times 10^{-11}$ cm is the Compton wavelength and $r_0 = \frac{e^2}{m_e c^2} = 2.818 \times 10^{-13}$ cm is the classical electron radius. At an energy of 1.8 GeV, the polarization time of an electron beam in the VEPP-4M storage ring is ~100 h. Nevertheless, the presence of the VEPP-3 booster ring with a substantially smaller orbit radius R and a polarization time of ~1 h helps obtain polarized beams for use in the VEPP-4M.

The layout of the equipment for measuring the energy of the VEPP-4M beam using the RD method [6] is shown in Fig. 2. The beam is depolarized by means of a kicker—two asymmetric strip lines enclosed in a vacuum chamber at its top and bottom walls. A running TEM wave propagating along the beam is produced in the line. Its frequency varies according to the linear law in a range deliberately covering the value of the expected spin precession frequency. The sinusoidal signal of the depolarizer on the TEM wave is produced by the precision synthesizer developed by the BINP with a limiting resolution for the frequency tuning step of better than 6×10^{-7} Hz.

The effect of intrabunch particle scattering (the Touschek effect) is used to detect a beam depolarization event. The counting rate of scattered electrons, which is spin-dependent, is measured by two pairs of scintillation counters located in the vacuum chamber segment with a cylindrical cross section. The counters of each pair are introduced into the aperture in a horizontal plane on both sides and are used to detect electrons scattered around the circumference of the ring. The coincidence circuit for events detected in the counters of a pair is used to suppress uncorrelated noise.

The expression for counting rate of scattered particles $\dot{N}$ can be presented in the form [7]:

$$\dot{N} = \frac{\sqrt{\pi}r_0^2 c N_b^2}{\gamma^5 V_b (c\sigma_p/E)^3}(a + bP^2),$$
$$a = a(\varepsilon_1,\varepsilon_2), \quad b = b(\varepsilon_1,\varepsilon_2), \quad \varepsilon_{1,2} = \left(\frac{\Delta p_{1,2}}{\gamma\sigma_p}\right)^2, \quad (5)$$
$$\Delta p_1 = \Delta p_1(A), \quad \Delta p_2 = \Delta p_2(A_g),$$

where P is the degree of beam polarization, N_b is the number of particles in a bunch, V_b is the bunch volume in the laboratory system, σ_p if the spread of the transverse momentum in the beam, a and b ($b < 0$) are the evaluated functions dependent on the lower (Δp_1) and upper (Δp_2) limits on the transferred momentum, A is the distance from the counter to the orbit, and A_g is the geometrical aperture of the accelerator.

From Eq. (5), it follows that the counting rate of scattered electrons changes upon depolarization. In particular, the counting rate at the VEPP-4M storage ring changes by 1–3%. Measurement of a change in the counting rate as small as this is complicated by time instabilities of the beam, the influence of which is approximately equal in value to the useful effect. Therefore, detected are scattered particles from two bunches spaced apart by half the orbital period, one of which is polarized and the other is not.

The scintillation counters inserted into the vacuum chamber measure the ratio of the counting rates of scattered electrons from the polarized ($\dot{N}_1$) and nonpolarized ($\dot{N}_0$) beams: $1 - \dot{N}_0/\dot{N}_1$. When depolarization happens, the observed ratio changes stepwise in proportion to the degree of polarization squared (Fig. 3). Knowing the depolarizer frequency at the instant of a stepwise change in the counting rate ratio, we can find the spin precession frequency and, according to Eq. (3), the mean beam energy.

The limiting accuracy of absolute beam energy calibration using the RD method is governed by the width

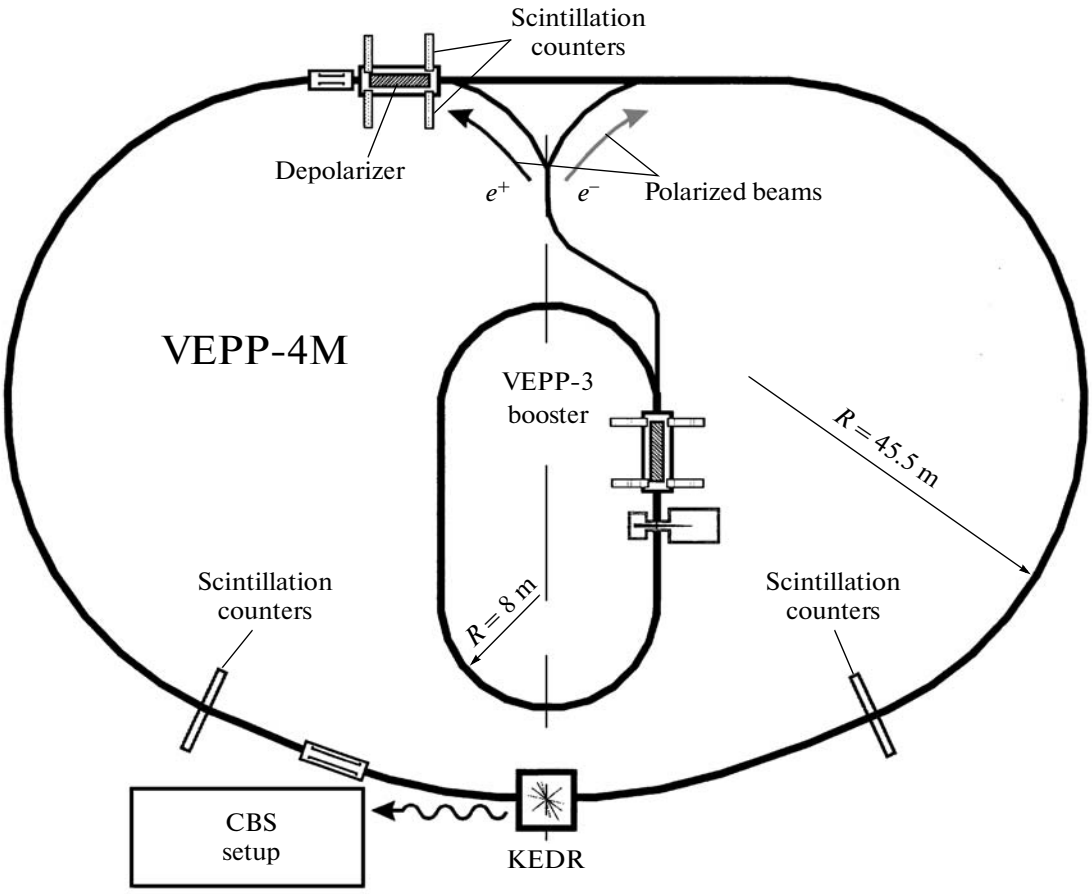

Fig. 2. Layout of the equipment for measuring the beam energy using the RD method.

of the spin line. According to estimates, this width is $\varepsilon_\nu \sim 5 \times 10^{-7}$ (~1 keV), which agrees with results of special experiments on the "ultrafine" scanning [8] at the VEPP-4M accelerator. The other parameter that limits the accuracy is an inverse time it takes for resonant depolarization to occur. When measuring the particle masses with the KEDR detector, this parameter was of the same order of magnitude with the spin line width.

The other sources of systematic errors of measurements using energy calibrations based on the RD method have been studied or currently being studied at the VEPP-4M. These sources include the following factors:

—breaking the law of proportionality between the spin frequency and the energy (the orbit is not flat or has a torsion) [9, 10];

—the dependence of the weighted-mean frequency of spin precession in a bunch on its current;

—the effect of small perturbations of the orbit (e.g., when orbits are separated in parasitic interaction points); and

—long-term stability of the energy between two successive calibrations (the temperature component, the stability of the accelerating RF system frequency, and the stability of the magnetic elements) [11].

To determine more precisely the error in measuring the energy in the center-of-mass system based on energy calibration data for only one (electron) beam, which is included into a final result of measurements of particle masses by the KEDR detector, the following factors were investigated:

—the compliance of the local energy at an interaction point with the mean energy over the storage ring, measured using the RD method (the asymmetry of radiation losses and the longitudinal particle acceleration in the field of the counter-propagating bunch);

—the agreement with the energy mean-weighted over the luminosity according to the RD method (the chromaticity of the β function, the effect of the separation at parasitic interaction points on the vertical dispersion at the main interaction point) [12]; and

—the correspondence of the energy of produced particles to the kinetic energy determined from the spin precession frequency (the potential in the beam) [13].

In high-energy physical experiments, it is necessary that the beam energy be known as the statistics is acquired, whereas energy calibration is not performed during data acquisition. The accuracy of energy measurements at the instant of calibration is 1 keV, but the actual energy during data acquisition differs from the

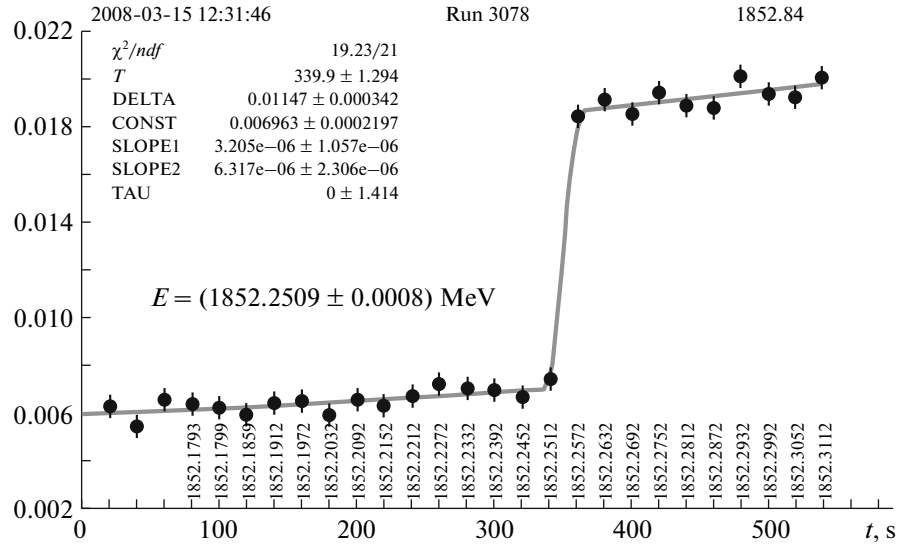

Fig. 3. Ratio of the counting rates from the polarized and nonpolarized bunches during depolarization.

measured value due to the instability of the storage-ring parameters in time. The energy was calculated using the following dependence on the accelerator parameters:

$$E_{beam} = \alpha_H H_{NMR}\left[1 + \alpha_T\left(T_{ring} - T_{NMR}\right)\right] f\left(T_{ring}, T_{cool}, T_{wall}\right) + A(t)\cos\left(\frac{2\pi t}{\tau_{day}} - \varphi(t)\right) + \delta E_{on}\exp\left(-t_{on}/\tau_{on}\right) + \delta E_{cycle}\exp\left(-t_{cycle}/\tau_{cycle}\right) + E_0\left(\Delta I_{mag}, t\right), \quad (6)$$

where H_{NMR} is the magnetic field measured by the NMR magnetometer in the calibration dipole magnet fed in series with the magnets of the VEPP-4M arcs; T_{NMR} is the temperature of the calibration magnet; T_{ring} and T_{cool} are the average temperatures of the ring and the cooler (air and water); T_{wall} is the temperature measured at a certain depth in the walls of the tunnel in which the accelerator is located, t is the current time; t_{on} and t_{cycle} are the times after the last switch-on of the magnetic system and the last magnetic cycle, respectively; and α_H, α_T, δE_{on}, δE_{cycle}, τ_{on}, and τ_{cycle} are the free parameters determined by fitting all energy calibrations performed in a certain collider's operating mode. Function $E_0(\Delta I_{mag}, t)$ includes the energy variations caused by relatively major changes in the current in some elements of the magnetic structure. The exponential members are responsible for the magnetic field relaxation after its switching-on and after a magnetization reversal cycle.

In the course of the whole experiment [14] (218 calibrations), the quasi-statistical accuracy of interpolation varied within the limits of 6–8 keV. Various versions of functions $f(T)$, $A(t)$, and $\varphi(t)$ were tested to estimate the systematic uncertainty of the resultant values for J/ψ- and $\psi(2s)$ mesons.

The use of the full form of parameterization (6) requires numerous energy calibrations without a substantial change in the operating mode of the accelerator. A simplified form of Eq. (6) with relatively short time intervals was used in the experiments aimed at measuring the masses of $\psi(3770)$ and D mesons and a τ lepton. The number of free parameters varied from four to seven. An interpolation accuracy of 10–15 keV was attained in scanning narrow resonances and 15–30 keV in scanning $\psi(3770)$ and the τ-lepton threshold.

Compton Backscattering

This method was used for the first time at the BESSY-I synchrotron radiation source (Berlin, Germany) [15]. The CBS method was implemented at the VEPP-4M in 2005 for the first time for colliding-beam facilities; since that time, it has been a routine tool for monitoring the beam energy [16].

The CBS method is based on the fact that the maximum energy of a scattered photon is unambiguously related to the electron and photon energies before scattering:

$$\omega = \omega_0 \frac{1 - \beta\cos\alpha}{1 - \beta\cos\theta + \frac{\omega_0}{E}(1 - \cos\Theta)}, \quad (7)$$

where ω and ω_0 are the photon energies before and after scattering, respectively; E and $\beta = v_e/c$ are the energy and the Lorentz factor of the electron before scattering; α is the angle between the photon and the electron before scattering; θ is the angle between the momenta of the primary electron and scattered photon; and Θ is the angle between the momenta of the primary and scattered photons (Fig. 4).

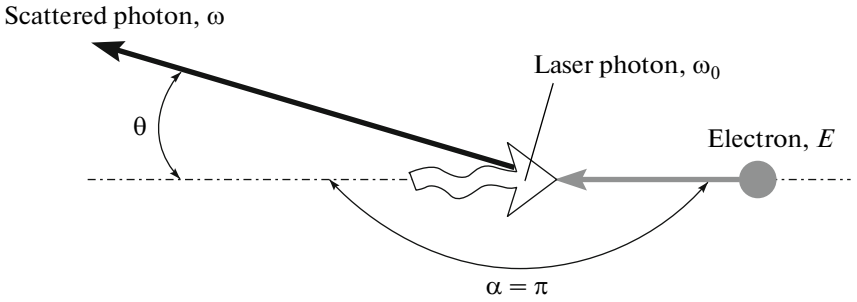

Fig. 4. Kinematics of Compton scattering.

Maximum energy of the scattered photon ω_{max} corresponds to the direction of the primary electron momentum ($\theta = 0$, $\Theta = \alpha$):

$$\omega_{max} = \omega_0 \frac{1-\beta\cos\alpha}{1-\beta+\frac{\omega_0}{E}(1-\cos\alpha)}. \quad (8)$$

In the case of $\alpha = \pi$ (a head-on collision), the energy of the scattered photon reaches the maximum possible value ω_{max}:

$$\omega_{max} = E^2 / \left(E + \frac{m^2}{4\omega_0}\right). \quad (9)$$

The energy spectrum of scattered photons is presented in Fig. 5. The dependence of the scattering cross section on the photon energy is shown with a solid line, and the photon scattering angle θ in terms of θ_c ($\theta_c \sim 1/\gamma \equiv m/E$) versus the photon energy is shown with dots. For both plots, the primary photon energy is $\omega_0 = 0.12$ eV, the electron energy is $E =$ 1777 MeV, and the interaction angle is $\alpha = \pi$.

Analysis of Fig. 5 shows that photons with maximum energy ω_{max} are scattered in a direction along the momentum of the primary electron and form a sharp edge in the energy spectrum, which offers a chance to determine ω_{max} from the measured spectrum. It is apparent that, to perform this task, primary photon energy ω_0 must be constant and well-known. Such photons can be produced by a laser with a narrow emission spectrum. In practice, it is reasonable to consider the interaction between the laser and electron beams, having in mind that the E and ω_0 values correspond to the mean energies of interacting electrons and photons. Therefore, measuring the average value of ω_{max}, one can determine the mean electron energy in the beam:

$$E = \frac{\omega_{max}}{2}\left(1 + \sqrt{1 + \frac{m^2}{\omega_0\omega_{max}}}\right) \cong \frac{m}{2}\sqrt{\frac{\omega_{max}}{\omega_0}}. \quad (10)$$

A COHERENT GEM Select 50 CO_2 laser is used at the VEPP-4M as a source of monochromatic photons. The laser generates by 10P20 transition with photon energy $\omega_0 = 0.117065223$ eV ($\lambda = 10.591$ μm). This wavelength has been selected so that the maximum energy of Compton γ rays is in the range of 4–7 MeV, which corresponds to the measured beam energy range of 0.5–2.0 GeV. The width of the laser spectrum does not exceed $\sigma_{\omega_0}/\omega_0 \le 3.5 \times 10^{-6}$, and the mean energy of laser beam photons is assumed to be constant with an accuracy of $\Delta\omega_0/\omega_0 \le 10^{-8}$. The power of continuous laser radiation is ~50 W (TEM_{00}). Using the system of lenses and mirrors, the laser beam is focused and injected through a window (ZnSe) into the vacuum chamber of the storage ring, where it interacts with the electron beam at zero angle.

A high-purity germanium (HPGe) detector is used to measure the spectrum of Compton γ rays. At an operating temperature of ~90 K, the HPGe conductivity is rather low, which allows the detector to be used at high cutoff voltages (1.5–3.5 kV) and guarantees a high efficiency in collecting the charge released by ionizing radiation inside the detector. The mean energy required for production of a single electron–hole pair in germanium is 2.95 eV (at $T = 90$ K), which determines its excellent spectrometric properties. A coaxial HPGe detector with an active volume of ~120 cm^3 and a total absorption efficiency of 5% for

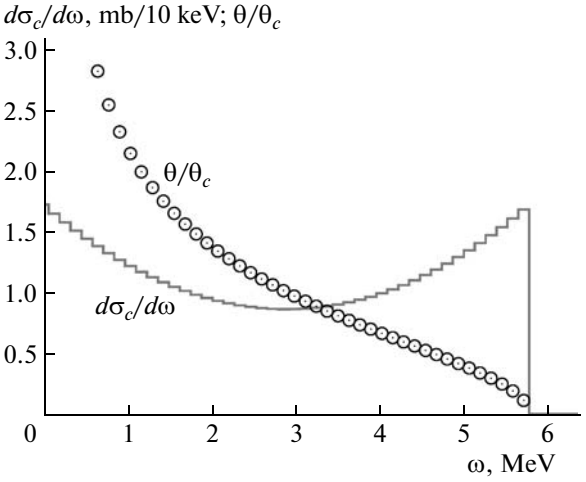

Fig. 5. Energy spectrum of scattered photons (curve) and dependence of the scattering angle on the photon energy (dots).

Table 2. Isotopes for HPGe detector calibration

Source	Half-life period	E_γ, keV	$\pm\Delta E_\gamma$, eV
^{24}Na	14.96 h	1368.625	5
		2754.008	11
^{60}Co	5.2714 yr	1173.228	3
		1332.492	4
^{137}Cs	30.07 yr	661.657	3
^{228}Th (decay products)	1.9131 yr	583.187	2
		2614.511	10

photons with energies of 5–6 MeV is used at the VEPP-4M. Radioactive γ-ray sources with the parameters presented in Table 2 are used to calibrate the energy scale of the detector.

The average counting rate of γ rays emitted by the calibration isotopes is ~1 kHz. The counting rate of Compton γ rays depends on the conditions of data acquisition, being 10^3 s^{-1} on the average. For the beam energy to be measured with a required accuracy, about 5 million events must be detected, which takes 5–30 min, depending on the γ-ray flux density. The energy spectrum of Compton γ rays measured at the VEPP-4M collider is shown in Fig. 6.

The Compton edge in a spectrum is fitted by the function with six parameters:

$$g(x, p_{0\ldots5}) = \frac{1}{2}[p_4(x - p_0) + p_2]\mathrm{erfc}\left(\frac{x - p_0}{\sqrt{2}p_1}\right) - \frac{p_1 p_4}{\sqrt{2\pi}}\exp\left[-\frac{(x - p_0)^2}{2p_1^2}\right] + p_5(x - p_0) + p_3 . \quad (11)$$

The visible width of the spectrum edge (Fig. 6b) results from the energy spread in the electron beam and the energy resolution of the HPGe detector. The contribution of the latter factor is measured using the calibration curve shown in Fig. 7. Thus, the mean electron energy and the energy spread of particles in the beam are measured at once. When processing the spectrum, the monochromatic lines of the calibration γ-ray sources are used for absolute calibration of the scale and for determining the energy resolution of the HPGe detector.

The main sources of systematic errors in measuring the beam energy at the VEPP-4M using this method are as follows:

—the necessity to extrapolate the energy scale from the calibration line with the maximum energy (2.6–2.7 MeV) to the energy of the Compton edge (5–6 MeV);

—a distortion of the full-energy peak in the HPGe detector spectrum at high beam intensities; and

—possible shift of the measured energy from the mean beam energy due to a high horizontal dispersion function ($\psi_x = 89$ cm) in the region of electron beam interaction with laser radiation.

In the course of data acquisition at energies near the τ-lepton production threshold in 2005–2007 ($E = 1777 \pm 5$ MeV), 153 calibrations of the beam energy were simultaneously performed using the RD and CBS methods. The experimental results are in agreement with an accuracy of ~50 keV or $\Delta E/E \sim 3 \times 10^{-5}$.

The typical time dependence of the accelerator energy calculated by the VEPP-4M parameters is shown in Fig. 8; the energy values measured using the RD and CBS methods are also plotted in the figure. It is apparent that, after the energy is lowered, the guiding magnetic field is stabilized within 3 h, which results in energy drift by a value of ~0.1 MeV. Further energy drift, which is slower, can be attributed to the temperature drift.

THERMAL STABILIZATION SYSTEMS

The relative accuracy of energy calibration in experiments at the VEPP-4M reaches a record-breaking value of 10^{-6}. Investigations of all factors affecting the accuracy of beam energy measurements and contributing thereby to the systematic error of particle mass measurements showed that the following factors are of the highest significance:

—a variation in the geometrical dimensions of the magnets though the instability of the ambient temperature;

—a variation in the middle radius of the storage ring due to the thermal movement of the tunnel in which the accelerator is located;

—a variation in the temperature of the water that cools the magnetic elements of the accelerator; and

—the long-term instability and 50-Hz ripple of the magnets' power sources.

The strongest effect on the beam energy is exerted by thermal expansion of the combined magnets in the VEPP-4M semirings, which causes the integral of the magnetic field to vary. The magnets are cooled with distillate circulating over a closed loop. The distillate heated by the magnets is cooled in the heat exchanger by service water, the temperature of which depends on a variety of external factors (e.g., the ambient temperature, the humidity, and the cooling conditions in the cooler) and is therefore liable to substantial diurnal and seasonal variations. The diurnal variations in the beam energy caused by ambient temperature fluctuations are shown in Fig. 9.

To maintain the temperature of the VEPP-4M magnets within the predetermined limits without regard to external factors, a system stabilizing the distillate temperature has been developed and placed in operation. The temperature of the distillate and the service water at the inlet and outlet of the heat exchanger is measured by precision temperature sensors, and temperature data are transmitted by means

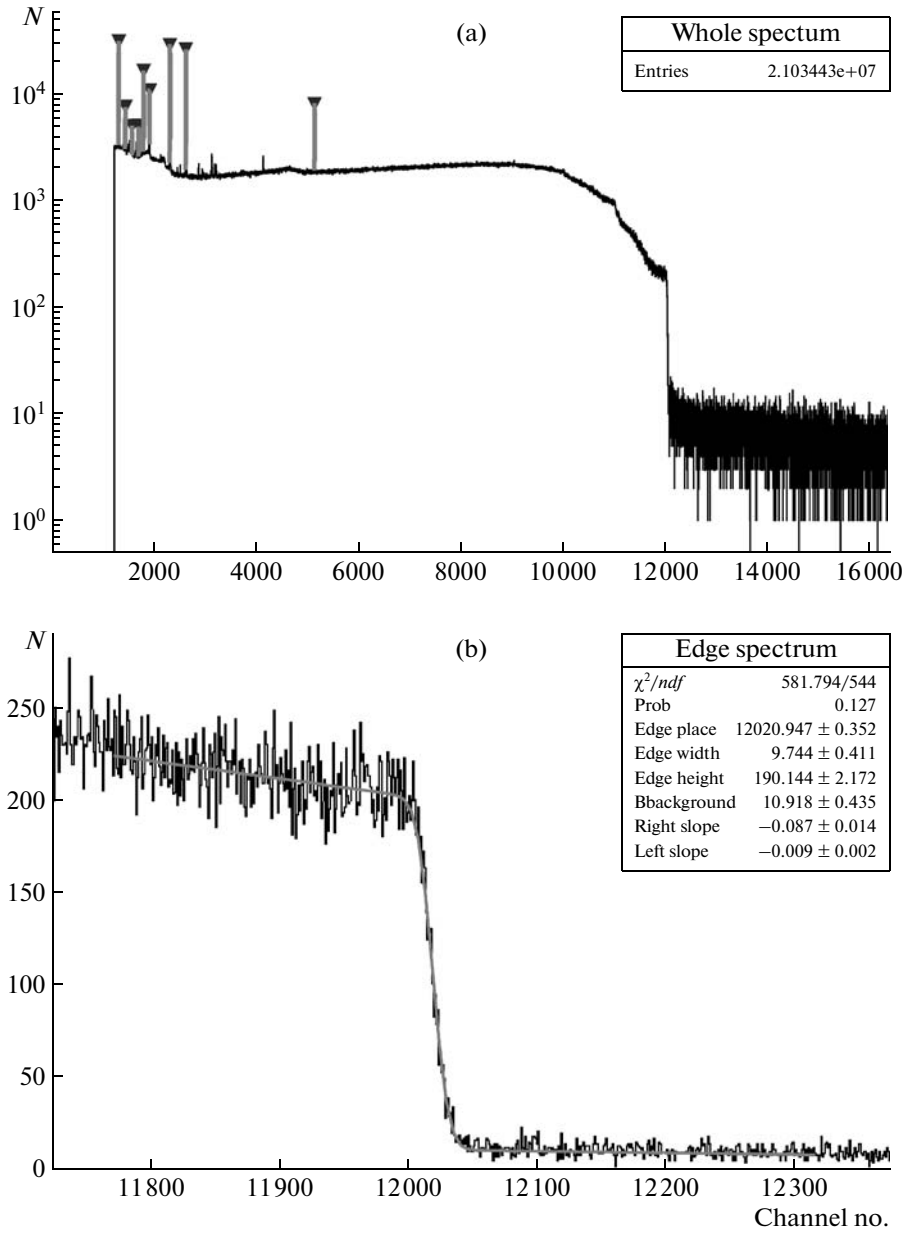

Fig. 6. (a) Compton γ-ray spectrum and (b) its edge on the expanded scale.

of a controller to a computer included in the control system of the VEPP-4 complex. A service water flow in the heat exchanger and, therefore, the heat-exchange efficiency are regulated with the aid of a controlled valve, which opens and closes in response to a command arriving from the control program analyzing the measured temperatures. The system efficiency is illustrated by Fig. 10, in which the diurnal fluctuations of the service water and distillate temperatures are plotted. The amplitude of the diurnal fluctuations of the magnet-cooling distillate is ~0.1°C, which is a factor of ~10 smaller than when the thermal stabilization system is the off state.

A mode of operation with two electron and two positron bunches has been used in high-energy physical experiments on the VEPP-4M electron–positron collider. The instability of the longitudinal beam motion responsible for high-amplitude phase oscillations is a side effect of the multibunch mode. Phase oscillations lead to a sharp decrease in the luminosity and the beam lifetime. Moreover, incidence of beam particles on the drift chamber of the KEDR detector may initiate high-voltage breakdowns and damage the drift chamber.

The instability is caused by resonance excitation of higher-order modes of the accelerating cavities by the beam. Each of the five cavities has three controlled

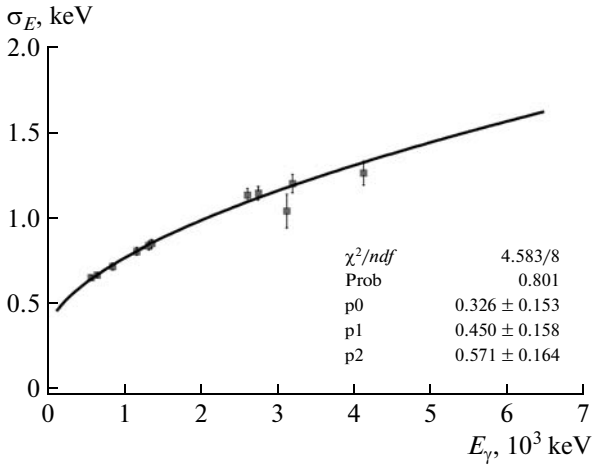

Fig. 7. Energy resolution of the HPGe detector vs. the γ-ray energy (dots) and fitting function $R(x, p_{0\ldots2}) = p_0 + p_1 x^{p_2}$ (a curve).

mechanisms to suppress these modes. There are regions of stable beam motion that correspond to certain tuning of the mechanisms suppressing the higher-order modes. Nevertheless, a change in the cavity temperature is followed by a change in the cavity dimensions, which result in a shift of the resonance frequencies of the higher modes and, therefore, in development of the beam motion instability.

The cavities are cooled by a separate distillate loop, which has a high resistivity. To stabilize the temperature of the cavities, a system based on controlled distillate heaters has been developed; it helps maintain the preset temperature with an accuracy of 0.05–0.10°C at a flow rate of ~10 l/min. The temperature is measured at the heater input and output by means of temperature sensors with a sensitivity of ~10 mV/°C. Results of temperature measurements are fed into the offline ADAM microprocessor, which controls the heating power and switches the heater on or off by means of semiconductor switches. The ADAM microprocessor is connected to a computer included in the control system of the VEPP-4 complex. The control computer is used to monitor and load the ADAM microprocessor, which operates in the offline mode after loading.

Figure 11 presents the 16-h temperature dependences of the distillate that cools the cavities, with the thermal stabilization system being switched off and on. The use of the thermal stabilization system has made it possible to lower the diurnal temperature fluctuations from 2–5 to 0.1–0.2°C and, as a consequence, the rate of occurrence of phase oscillations in the experimental mode has been reduced by a factor of ~100.

A MULTIPINHOLE CAMERA

In high-energy physical experiments at the VEPP-4M collider with the KEDR detector, it is necessary that long-term stability of the beam orbit in the region near the interaction point be maintained. This is needed for reliable operation of important diagnostic devices, such as the luminosity monitor and the system for measuring the energy by Compton backscattering. However, the insufficient time resolution of the electronics of the beam position monitor makes it impossible to achieve the required accuracy in measuring the orbit in the situation when the electron and positron beams simultaneously circulate in the collider.

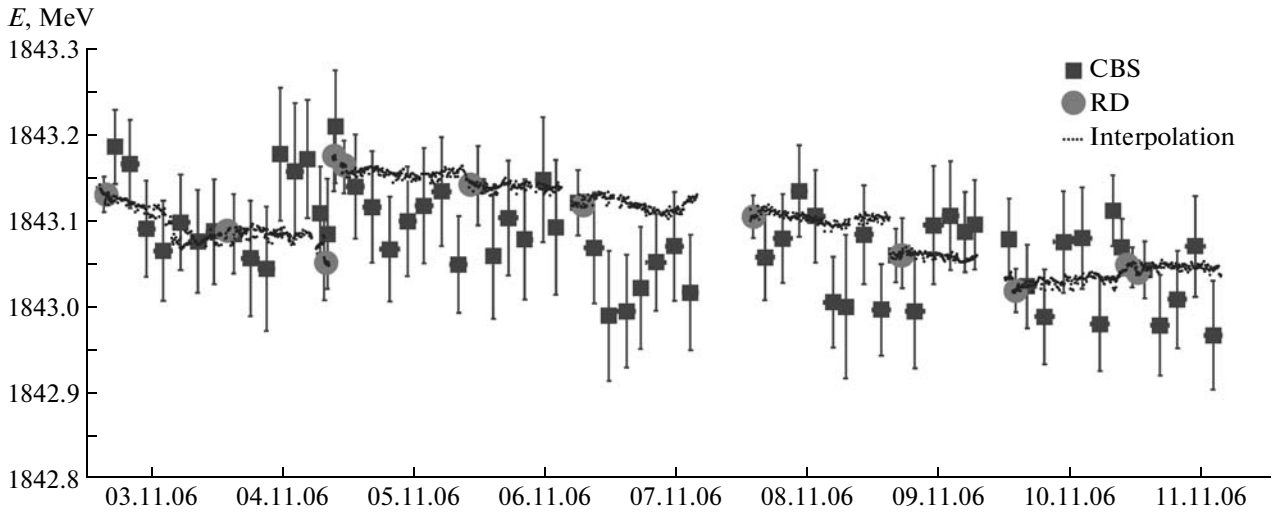

Fig. 8. Measurement and interpolation of the VEPP-4M beam energy.

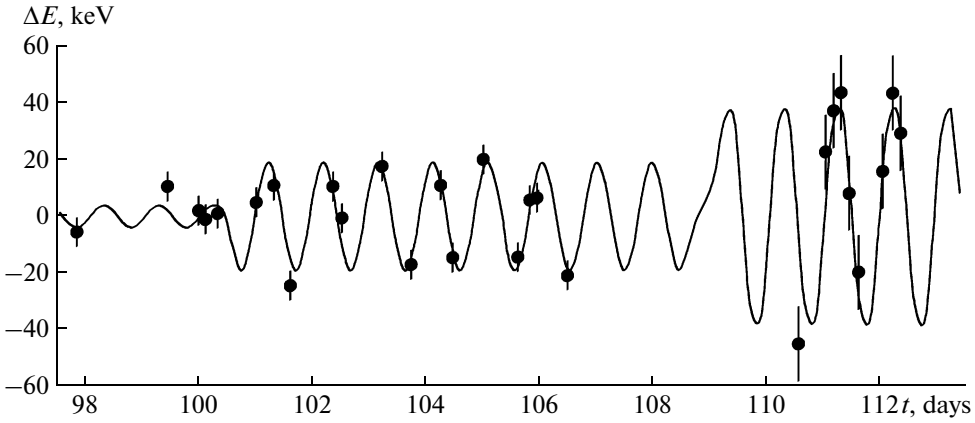

Fig. 9. Diurnal variations of the beam energy.

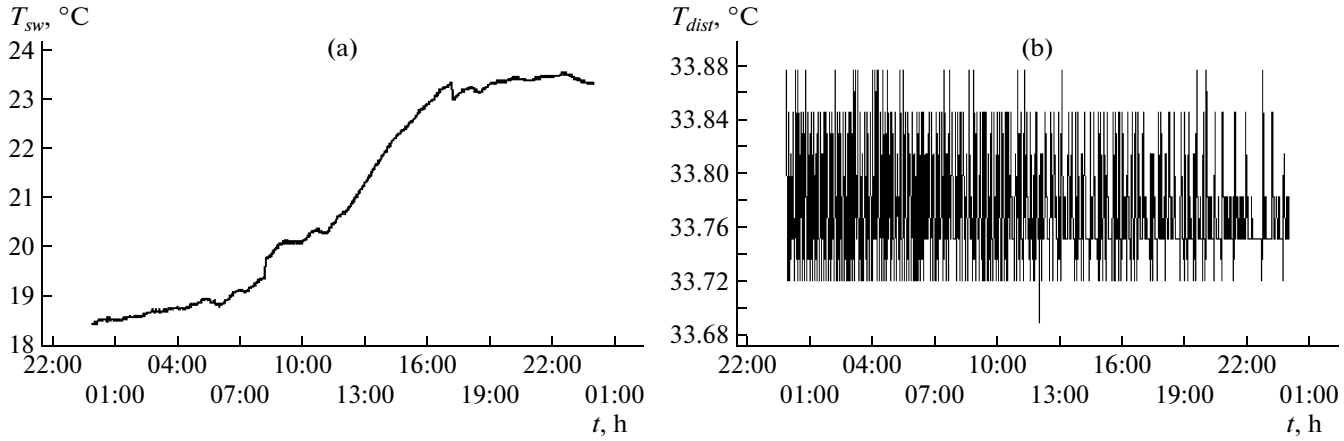

Fig. 10. Temperatures (a) of the service water T_{sw} and (b) VEPP-4M magnets-cooling distillate T_{dist}, measured over 24 h (with thermal stabilization).

An optical technique based on the use of a multipinhole camera has been proposed for stabilizing the orbit of the electron and positron beams in the NEM2 and SEM2 bending magnets adjacent to the interaction point. The X-ray multipinhole camera possesses geometrical properties similar to an ordinary pinhole camera for visible light. Passing through a small hole, light forms an inverted image of the source with a transformation ratio equal to D/d, where d is the distance from the source to the screen, and D is the distance from the screen to the recording device (a CCD array).

If a metal screen has a few holes located in line with a separation of $\sim 3\sigma_y$ (σ_y is the transverse beam size), we will have an instrument permitting simultaneous measurements both of the transverse location of the beam and its angle of inclination at the radiation point. The spacing between the outer holes must be $\sim 3d\psi$, where ψ is the angular divergence of synchrotron radiation and d is the distance from the radiation point to the screen.

The idea of simultaneous measurements of the beam's transverse displacement and angle of inclination are illustrated in Fig. 12. If the transverse cross section and the angle of inclination are zero, X-ray synchrotron radiation creates a beam image at the metal screen, so that the center of the image is located exactly in the middle between two outer holes and the superposition of images formed by holes forms a symmetric figure on the phosphor (see Fig. 12a). The transverse displacement of the beam without an angular displacement causes all images on the phosphor and, therefore, their envelope to be shifted by value $y_1 = -yD/d$, see Fig. 12c. Inclination of the beam at angle φ without a displacement in the transverse plane results in a shift of only the envelope of the beam images by value $y_2 = \varphi d$, since the images themselves remain at their sites, but their intensity changes (Fig. 12c).

Therefore, the basic algorithm for determining the beam displacement by the coordinate and the angle includes the following operations:

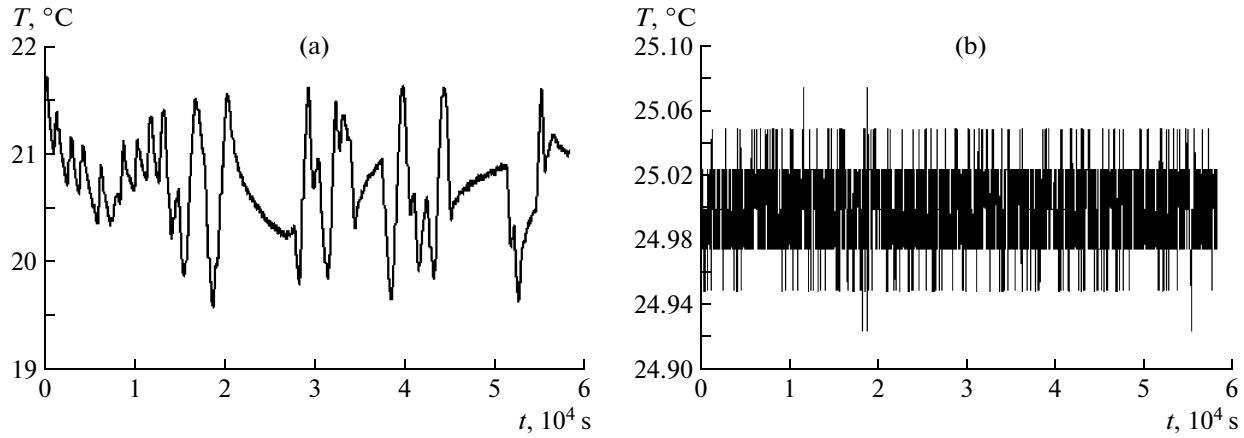

Fig. 11. Distillate temperature with the thermal stabilization system being (a) switched off and (b) on.

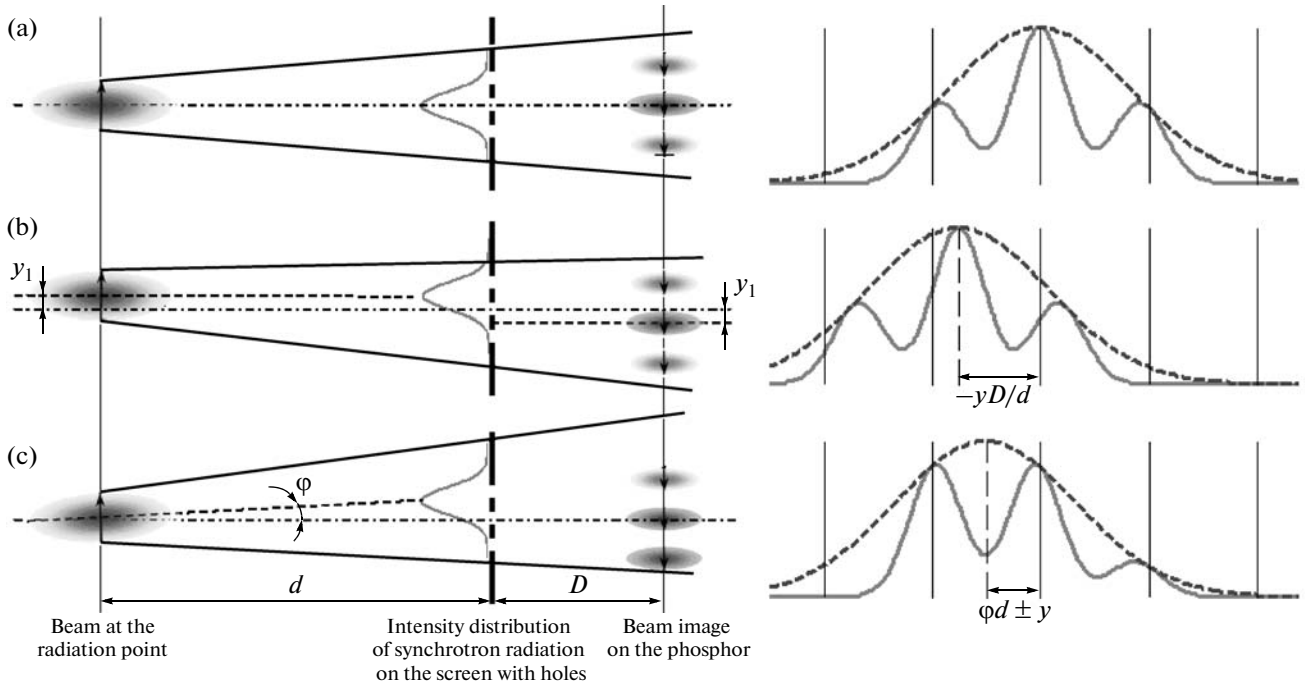

Fig. 12. Principle of measurements of the transverse coordinate and the ingle of inclination of the beam.

(i) measuring transverse displacement y_1 of the beam images on the phosphor;

(ii) measuring displacement y_2 of their envelope;

(iii) calculating transverse displacement of the beam at the radiation point $y = -y_1 d/D$; and

(iv) calculating angle of inclination $\varphi = (y_2 \pm y)/d$ (sign "+" corresponds to the case of $y_2 < y$, and sign "−" corresponds to the case of $y_2 > y$).

Soft X-ray radiation from the bending magnet, ejected outward through a beryllium foil, is used to construct the beam image by the multipinhole camera. The spectral composition of radiation is such that it is almost fully absorbed in the atmosphere at a distance of ~1.5 m. In this connection and, in addition, in order to avoid damage to the beryllium foil, radiation is ejected toward the phosphor through a tube pumped down to a rough vacuum. The phosphor produced from ZnS converts an X-ray image into visible light; the beam image is thereafter transferred by the objective lens to the CCD array and read out into a computer (Fig. 13a). Processing of measured data yields the envelope of the beam images (Fig. 13b), which is used to determine the transverse displacement and angle of inclination of the beam at the radiation point.

The existing configuration of the instrument allows determination of solely the vertical angle. In the hori-

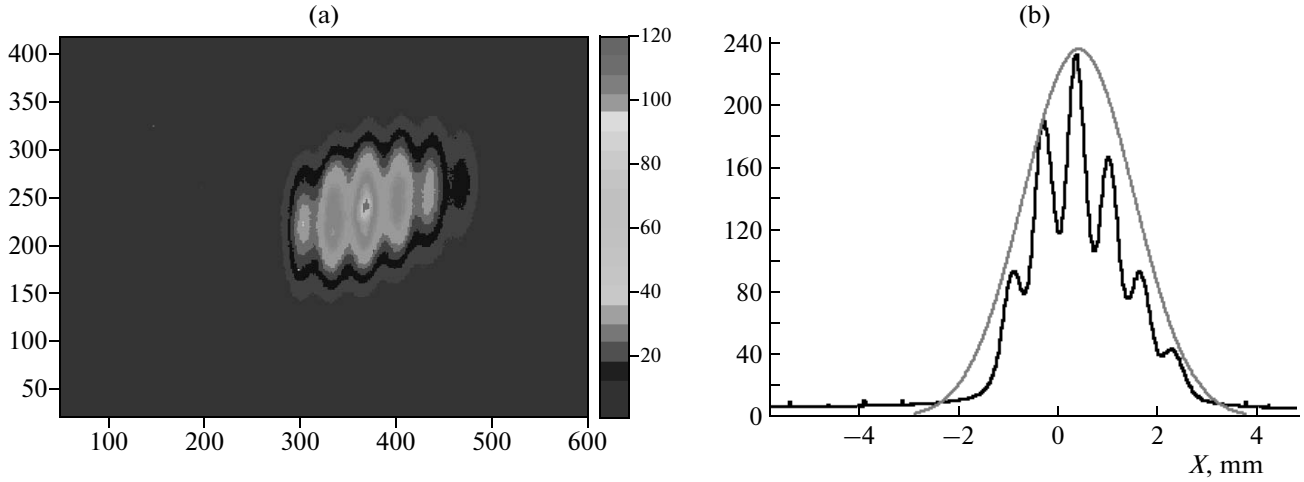

Fig. 13. (a) Beam image obtained using the multipinhole camera and (b) envelope reconstructed by the experimental results.

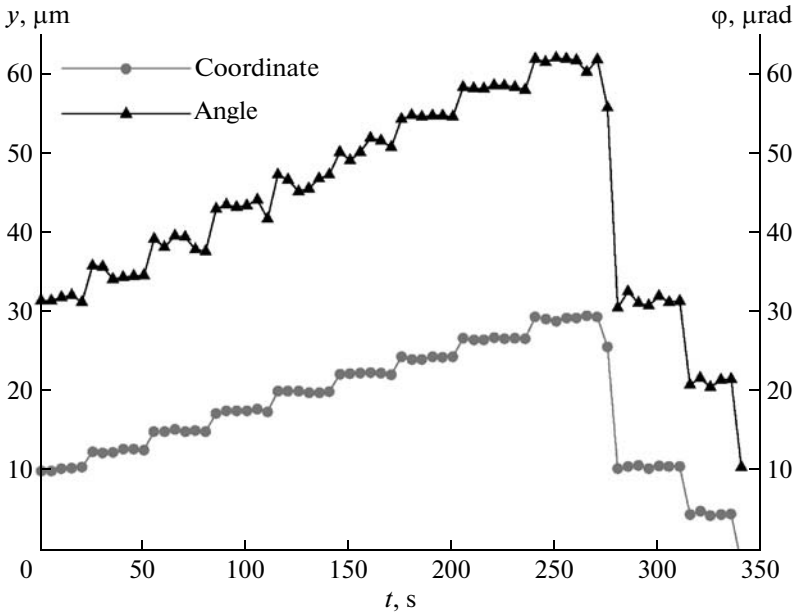

Fig. 14. Measured resolution of the multipinhole camera.

zontal direction, only the displacement can be monitored, but even this fact is of great importance for maintaining the stability of the beam energy. According to theoretical estimates, the spatial and angular resolutions of the instrument are expected to be 20 μm and 50 μrad, respectively. The measured resolution of the multipinhole camera as a function of the coordinate and the angle are shown in Fig. 14. The vertical position (dots) and the angle (a curve) of the beam were varied using an orbit corrector and monitored by electrostatic sensors of the beam position.

Today, we do not pose the problem of measuring the vertical and radial beam sizes at the observation point, but, theoretically, this is possible.

CONCLUSIONS

A system of particle energy measurements using the resonant depolarization method with record-breaking relative accuracy has been built at the VEPP-4M electron–positron collider. The procedure for reconstructing the beam energy between calibrations with an accuracy of 10^{-5} has been developed. Measurements of particle energies using the RD and CBS methods make it is possible to conduct precision high-energy physical experiments at the VEPP-4–KEDR complex in spite of the loss of luminosity relative to the modern colliders. The masses of J/ψ- and $\psi(2s)$ mesons were measured at the VEPP-4 complex with an accuracy a factor of 3–4 better than the world-

average value. These masses are now among the ten most precisely known particle masses measured over the whole of the history of physics. In addition, the masses of $\psi(3770)$, $D^{\pm}$ meson, and τ lepton have been measured with the best accuracy worldwide.

A system stabilizing the temperature of the distillate that cools the combined magnets of the semirings has been developed and placed in operation in order to improve the stability of the beam energy in the VEPP-4M collider. A thermal stabilization system for RF cavities has been developed to reduce the operating-time loss due to occurrence of phase oscillations. Measurements demonstrated a significant decrease of temperature fluctuations in the cavities and, therefore, stabilization of the longitudinal beam motion.

Simultaneous measurements of the beam's transverse displacement and angle of inclination using the X-ray multipinhole camera have been used to improve the accuracy in measuring the orbit of the beams near the interaction point in high-energy physical experiments at the VEPP-4M with the KEDR detector.

REFERENCES

1. Skrinsky, A.N., *Nucl. Instrum. Methods Phys. Res. A*, 2009, vol. 598, p. 1.
2. Anashin, V.V., Aulchenko, V.M., Baibusinov, B.O., et al., *Nucl. Instrum. Methods Phys. Res. A,* 2002, vol. 478, p. 420.
3. Anashin, V.V., Aulchenko, V.M., Baldin, E.M., et al., *Nuclear Physics B, Proceedings Supplements*, 2008, vols. 181–182, p. 353.
4. Anashin, V.V., Aulchenko, V.M., Baldin, E.M., et al., Nuclear Physics B, *Proceedings Supplements*, 2008, vols. 181–182, p. 311.
5. Bukin, A.D., Derbenev, Ya.S., Kondratenko, A.M., et al., *Preprint of Inst. of Nucl. Phys., Siberian Branch, Acad. of Sci. of the USSR*, Novosibirsk, 1975, no. 75-64; *Trudy V mezhdunarodnogo simpoziuma po fizike vysokikh energii i elementarnykh chastits* (Proc. of V Int. Symp. on High Energy and Particle Physics, Warsaw, 1975), Dubna, 1975, p. 138.
6. Blinov, V., Bogomyagkov, A., Cherepanov, V., et al., *Beam Dynamics Newsletter*, 2009, no. 48, p. 181.
7. Nikitin, S. and Nikolaev, I., *Proc. of EPAC-2006*, 2006, P. 1184.
8. Blinov, V., Bogomyagkov, A., Karpov, G., et al., *Beam Dynamics Newsletter*, 2009, no. 48, p. 207.
9. Bogomyagkov, A., Nikitin, S., and Shamov, A., *Proc. of RuPAC-2006*, Novosibirsk, 2006, p. 153.
10. Nikitin, S., *Proc. of RuPAC-2006*, 2006, p. 151.
11. Bogomyagkov, A.V., Karnaev, S.E., Kiselev, V.A., et al., *Proc. of EPAC-2002*, Paris, 2002, p. 386.
12. Bogomyagkov, A., Nikitin, S., Nikolaev, I., et al., *Proc. of the 22nd PAC*, Albuquerque, 2007, p. 63.
13. Bogomyagkov, A., Nikitin, S., Telnov, V., and Tumaikin, G., *Proc. of APAC-2004*, Gyeongju, Korea, 2004, p. 276.
14. Aulchenko, V.M., Balashov, S.A., Baldin, E.M., et al., (KEDR Collab.), *Phys. Lett. B*, 2003, vol. 573, p. 63, e-Print: hep-ex/0306050.
15. Klein, R., Kuske, P., Thornagel, R., et al., *Nucl. Instrum. Methods Phys. Res. A*, 2002, vol. 486, p. 545.
16. Blinov, V.E., Kaminsky, V.V., Levichev, E.B., et al., *Beam Dynamics Newsletter*, 2009, no. 48, p. 195.